

Computer Simulation of the Pioneer 10 Microwave Occultation Experiment

STEVEN G. UNGAR

*Institute for Space Studies, NASA Goddard Space Flight Center
New York, New York 10025*

As Pioneer 10 approaches the planet Jupiter, its trajectory will carry it behind the planet, as seen from the earth. The microwave telemetry signal from the spacecraft will then pass through the Jovian atmosphere on its way to the earth, and analysis of the effects of the atmosphere on the signal should yield information on the atmospheric structure. To help define the capabilities of this experiment and to aid the analysis of the real data, we have simulated the occultation experiment on a computer by using model Jovian atmospheres and a predicted trajectory. The results indicate that the useful depth of penetration of the microwave signal will be governed by ammonia absorption rather than superrefractivity. The experiment is apparently far more sensitive to variations in cloud top temperature than to variations in the hydrogen-helium ratio. Characteristic 'flashes' in the attenuation record of the signal may yield information on the location of the top of the Jovian convective zone.

Microwave occultation experiments have proven to be useful in sensing the atmospheres of terrestrial planets. Mariner 4, 6, 7, and 9 [Kliore *et al.*, 1965, 1969, 1972; Hogan *et al.*, 1972] carried occultation experiments that were successful in detecting and analyzing the tenuous atmosphere of Mars: Mariner 5 carried a dual-frequency experiment that sensed the ionosphere and dense atmosphere of Venus [Mariner Stanford Group, 1967; Kliore *et al.*, 1967].

Two spacecraft, Pioneer 10 and 11, have been launched toward Jupiter, the first nonterrestrial planet to be the target of scientific probes. Pioneer 10 was scheduled to arrive at the planet December 4, 1973, and Pioneer 11 is scheduled to arrive December 1974. An occultation experiment is planned for each spacecraft. This paper summarizes a computer simulation of the Pioneer 10 occultation experiment, using models of the Jupiter atmosphere, in an attempt to predict the more interesting areas for analysis of the actual data.

OCCULTATION EXPERIMENT

The occultation technique is based on the fact that as a radio wave passes through an atmosphere, it is bent and retarded. This happens because the atmosphere has an index of refraction n that is greater than 1 and that varies from place to place, i.e., has a nonzero gradient. An occultation of Pioneer 10 by Jupiter will take place when the spacecraft passes behind the planet, as seen from the earth. As Pioneer 10 approaches the limb of the planet, the radio line of sight from the earth to the spacecraft will begin to intercept the atmosphere of Jupiter. As the spacecraft moves closer to the planet (as seen from earth), the radio waves penetrate deeper into the atmosphere and are increasingly affected by refraction and retardation. In fact, by the time the spacecraft passes behind the planet the refraction effect is so pronounced that radio waves from the spacecraft are able to bend around the planet's limb, and radio contact will be maintained with the earth (provided that the signals are not too severely attenuated). The path of Pioneer 10, as seen from the earth, is shown in Figure 1.

In passing through the atmosphere the radio waves are affected three ways. First, they are retarded because the index of refraction of the atmosphere is greater than 1. It is useful to

define a quantity known as the refractivity, given by the formula

$$n = 1 + 10^6 N \quad (1)$$

where n is the index of refraction and N is the refractivity. The refractivity of an ideal nonpolar mixture of gases is proportional to its density. Any mixture of gases that has a density gradient will therefore also exhibit a gradient of N , and hence of n , which leads to the second effect of the atmosphere, namely, refraction or bending.

The third effect is attenuation, in which the energy of the signal is diminished by its passage. There are two principal components of attenuation. The first is due to defocusing, or spreading out of the signal due to differential refraction (this parameter is of major interest in stellar occultations). The second component is due to absorption of the signal by one or more atmospheric gases. For the Pioneer 10 experiment the principal absorbing gas is NH_3 , which suffers a pressure-enhanced inversion in the vicinity of the telemetry frequency (2292 MHz downlink).

By observing these three effects of the atmosphere on the radio signal—retardation, bending, and attenuation—it is possible to infer several properties of the atmosphere. Since the index of refraction is proportional to the density of the atmosphere, if we assume that the atmosphere consists of a mixture of gases, each of partial pressure p_i and common temperature T , we can write

$$N = C_i p_i / T \quad (2)$$

where the C_i are constants that may be determined in the laboratory, are generally different for each gas, and may be functions of frequency (i.e., the atmosphere may be a dispersive medium). In the case of Jupiter the major contribution to N comes from molecular hydrogen and helium. Thus if either the composition of the atmosphere or its temperature is known, knowledge of N allows us to calculate the other.

If either the temperature or the composition varies from place to place, N will also vary. From Snell's law it is known that an electromagnetic 'ray' tends to bend in the direction of increasing index of refraction. Mathematically, this can be written as

$$d\lambda/\lambda = d\rho/\rho \quad (3)$$

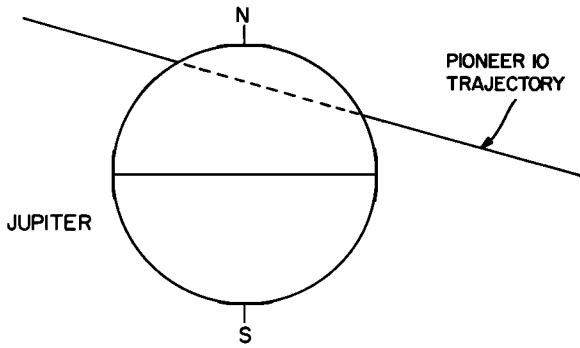


Fig. 1. Trajectory of the Pioneer 10 spacecraft as seen from earth.

where λ is the wavelength, ρ is the radius of curvature of the ray path, and the derivatives are taken in the direction of travel of the ray. The wavelength λ is related to frequency ν by $\lambda = v/\nu$, where v is the velocity of the wave. Because $v = c/n$, $\lambda = c/n\nu$ and $d\lambda = -(c/n^2\nu) dn$. Substituting these expressions into (3) and rearranging the terms result in

$$\rho = \frac{-n}{dn/d\rho} \quad (4)$$

which relates the radius of curvature of a ray to the index of refraction n and the derivative $dn/d\rho$. This derivative can be expressed as the sum of two terms; one is proportional to the horizontal gradient of n , and the other is proportional to the vertical gradient:

$$\frac{dn}{d\rho} = -\nabla n \frac{\rho}{|\rho|} = -\left| \frac{dn}{dr} \right| \cos \phi + \frac{1}{r} \frac{dn}{d\theta} \sin \phi \quad (5)$$

where r and θ are polar coordinates with origin at the center of the planet and ϕ is the angle between ρ (the radius of curvature vector) and r (the radius vector). The radius of curvature can now be written as

$$\rho = \frac{n}{\left| \frac{dn}{dr} \right| \cos \phi - (1/r) \frac{dn}{d\theta} \sin \phi} \quad (6)$$

Therefore the radius of curvature of a ray is found to be proportional to the index of refraction of the medium and inversely proportional to the gradient of the index of refraction. If the gradients are large, ρ will be small, and the ray will curve sharply; if they are small and n is large, the ray will follow a 'straight' trajectory.

In practice, the horizontal gradient term is usually much smaller than the vertical gradient term, and to simplify inversion of data, a spherically symmetric atmosphere is assumed, i.e., one in which horizontal gradients are zero. Equation 6 then becomes

$$\rho = \frac{n}{\left| \frac{dn}{dr} \right|} \cos \phi \quad (7)$$

Since atmospheric density increases with depth roughly exponentially, in a very thick atmosphere it is possible for the term dn/dr to become very large and the radius of curvature to become very small. If at some radial distance r the radius of curvature equals the radius r , a horizontal ray will remain horizontal and will circle the planet at a constant height ad infinitum. If the ray is bending slightly downward, it will pass into a region in which the radius of curvature is less than the radius r , and its downward angle will increase. The ray will then spiral ever closer to the planet until it finally strikes the

surface; or, in the case of a Jovian planet, it disappears into the planetary interior. Such rays are said to be trapped, and an atmosphere that traps rays in such a manner is said to be superrefractive.

The condition for superrefractivity is then

$$r = \rho = \frac{n}{dn/dr}$$

where r is the radial distance from the center of the planet. Since a ray trapped in a superrefractive atmosphere can never escape from the planet, it is impossible to use occultation to sense an atmosphere at superrefractive depths, and superrefractivity presents an absolute lower limit to the useful range of an occultation experiment.

SIMULATION OF THE EXPERIMENT

The Pioneer 10 occultation experiment has been simulated on the computer to define the information that can be obtained and to aid the analysis process once the real data are received. In performing the simulations we found the following parameters to be of interest: (1) the maximum depth of penetration, which is a function of the vertical density gradient of the atmosphere; it has been suggested that the Jovian atmosphere might be superrefractive, which would severely limit the usefulness of the occultation experiments; (2) the maximum attenuation, which is largely a function of the ammonia concentration; even if the rays are not trapped in the atmosphere, large attenuation due to ammonia absorption may cause loss of signal; (3) the sensitivity of the experiment to changes in gas composition and the temperature; and (4) any unusual features in the simulated signal that may be used to analyze the inversion of real data.

The simulations were performed on an IBM 360/95 computer by using models of the Jovian atmosphere developed by J. S. Hogan (private communication, 1973) and T. Encenaz at the Goddard Institute for Space Studies together with D. Gautier at the Meudon Observatory, Paris, France. Fifteen model atmospheres consisting of number density profiles for the gases H_2 , He, CH_4 , and NH_3 and a temperature profile were put into the computer. The fifteen profiles consisted of three sets of five profiles each. Within each set the cloud top temperature took values of 300° , 275° , 250° , 225° , and $200^\circ K$; the hydrogen-helium ratio (H_2/He) took the values 5:1 for the first set, 3:1 for the second, and 1:1 for the third. Temperature and H_2/He ratios were chosen so as to bracket generally accepted nominal values for these quantities.

The density profiles and temperature profile for the $250^\circ K$, 3:1 ratio profile are shown in Figures 2 and 3. The hydrogen and helium densities were used to construct a profile of refractivity as a function of altitude, and all five parameters were used to calculate the pressure-broadened ammonia absorption coefficient as a function of altitude.

The trajectory of the spacecraft in the vicinity of the planet was simulated by using trajectory data provided by the Pioneer project manager at the Ames Research Center in Moffett Field, California. Rays were 'launched' from the spacecraft toward the earth at 1-min intervals. The program traced the progress of the ray through the simulated Jovian atmosphere with a Snell's Law ray tracing routine and extrapolated the ray's progress toward the earth. The starting angle of the ray from the spacecraft was adjusted until the ray that intercepted the position of the receiver on the earth was

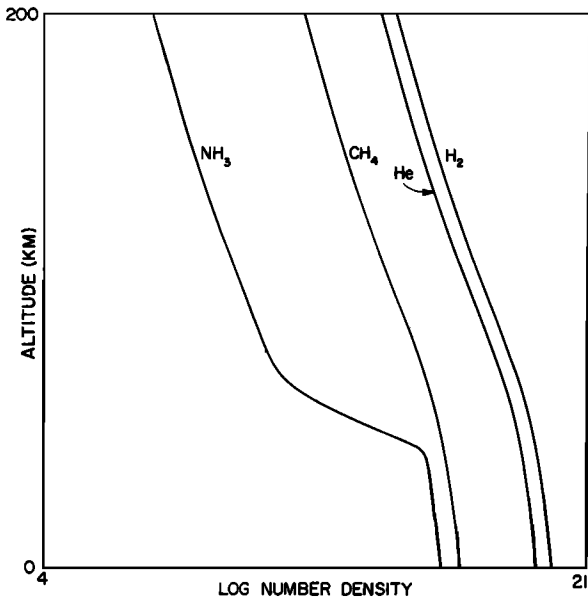


Fig. 2. Atmospheric composition for the Hogan model with a H_2/He ratio of 3:1 and cloud top temperature of 250°K. The top of the visible cloud layer is taken as $h = 0$.

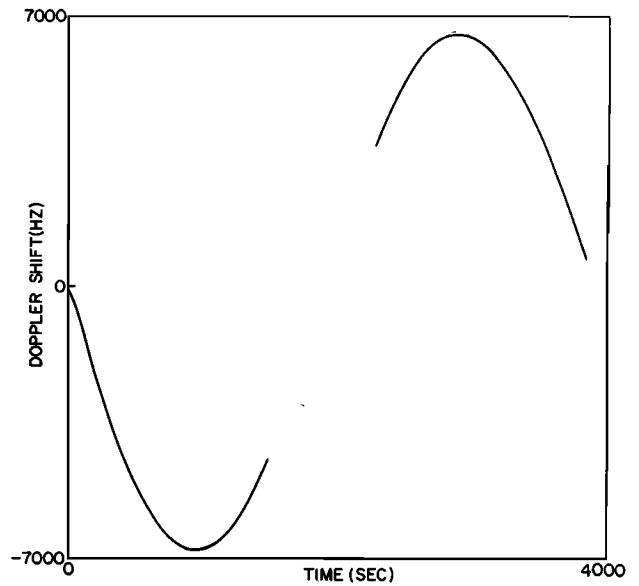


Fig. 4. Simulated Doppler residual obtained by ray tracing through the model of Figures 2 and 3.

found. Significant parameters such as attenuation, excess path length, and maximum depth of penetration were calculated and recorded for each ray to reach the earth. Records for the 250°K, 3:1 profile are shown in Figures 4 and 5.

ANALYSIS OF RESULTS

Analysis of the fifteen model Jovian atmospheres has been carried out with respect to the four areas of interest described above. The following significant results have been obtained.

1. In all of the profiles tested the maximum depth of penetration of the signal into the atmosphere is governed by factors other than superrefractivity; i.e., in no case is a ray trapped by the atmosphere. However, in some profiles the maximum depth of penetration was below the visible cloud deck, which was taken as $h = 0$ for these profiles. Since no data were available for these altitudes, ray tracing was not

possible. The breaks in the curves in Figures 4 and 5 represent the portion of the results that were not accessible in this simulation. It is not possible to tell whether a ray might not be trapped below the visible cloud deck; however, the results obtained indicate that the atmosphere is not superrefractive above the cloud deck.

2. In most of the models tested the ammonia absorption was found to be significant, leading to a major loss of signal at the deeper levels of penetration. In the result shown in Figure 5 the attenuation at the cloud deck is 185 dB. This is a typical value for attenuation at the maximum depth of penetration. Thus the ability of the experiment to sample deep in the Jovian atmosphere would appear to be limited not by superrefractivity but by attenuation due to ammonia absorption.

3. The relative sensitivity of the experiment to the changes in cloud top temperature and hydrogen-helium composition

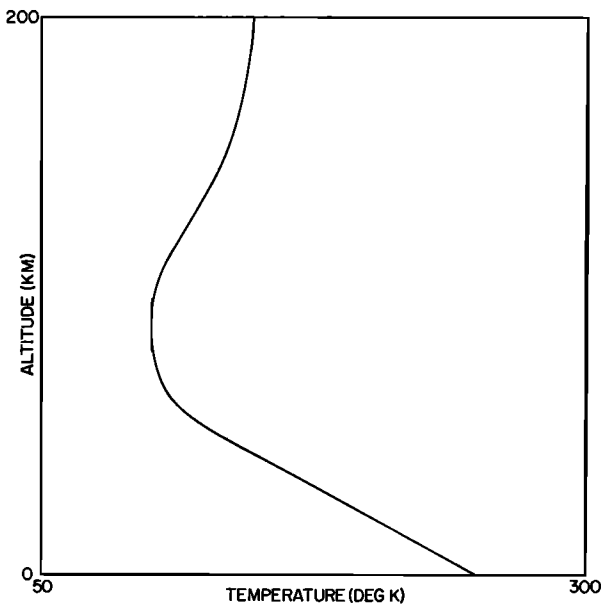


Fig. 3. Temperature profile for the model of Figure 2.

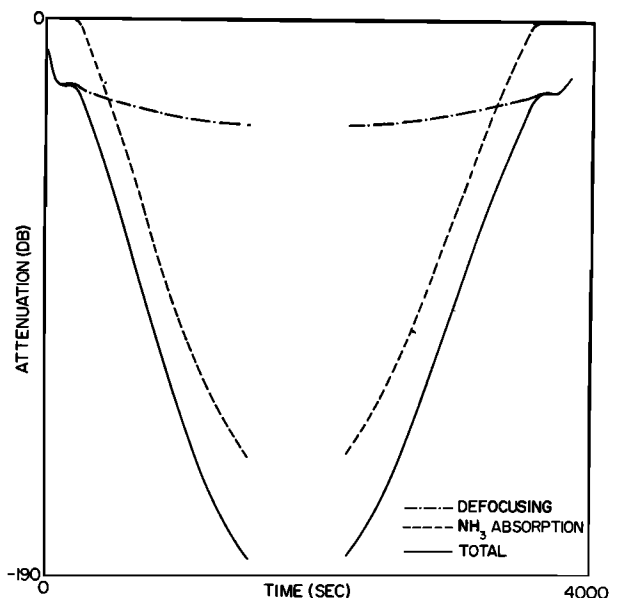


Fig. 5. Simulated attenuation record for the model of Figures 2 and 3.

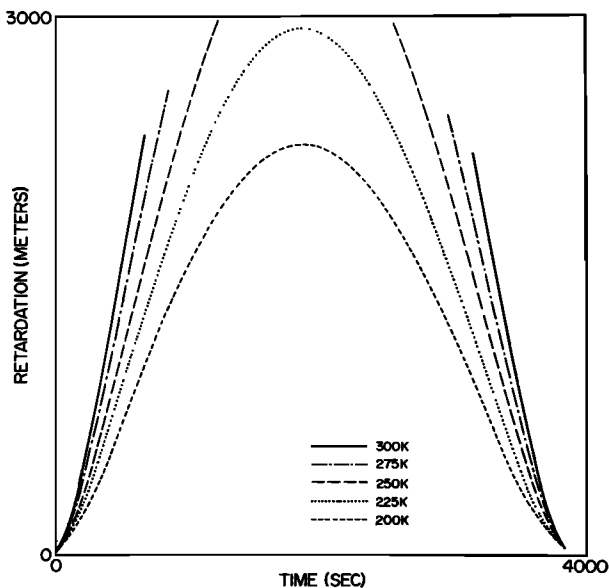


Fig. 6. Comparison of excess path length due to retardation as generated for five models, each with a H_2/He ratio of 3:1 and with cloud top temperatures as indicated.

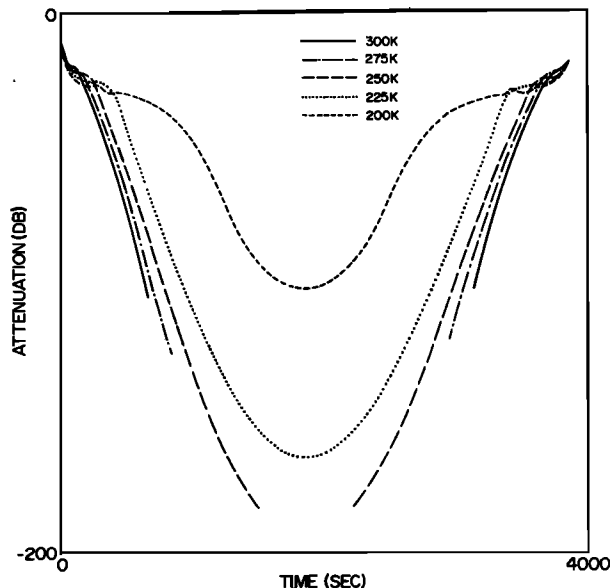


Fig. 8. Comparison of total attenuation as generated for five models, each with a H_2/He ratio of 3:1 and with cloud top temperatures as indicated.

is illustrated in Figures 6, 7, 8, and 9. Figure 6 shows five plots of retardation versus time for a H_2/He ratio of 3:1 and for each of the five cloud top temperatures. Excess path length due to retardation may be obtained from the total excess path length by applying standard inversion techniques to the experimentally obtained Doppler residuals. Figure 7 shows three plots of retardation versus time for a cloud top temperature of 250°K and for H_2/He ratios of 5:1, 3:1, and 1:1. It is clear that the experiment is far more sensitive to changes in cloud top temperature than it is to changes in gas composition. Figures 8 and 9 show similar plots for attenuation versus time. Once again, the experiment seems to distinguish more readily between different cloud top temperatures than between different compositions.

4. In the category of unusual features appearing in the

signal it was found that in the models tested a small 2-dB 'bump' appears in the attenuation record of the experiment (e.g., Figure 5). More detailed analysis (Figure 10) shows that this glitch is of fairly complex structure, resembling a damped sinusoid and appearing when the ray of closest approach first meets the top of the convection zone of the Jovian atmosphere. The top of the convection zone is characterized by a change in slope of the temperature profile as the energy transport mechanism of the atmosphere changes from convection to radiation. This appears as a small but marked change in the second derivative of the refractivity profile. (A similar phenomenon was noted by *Fjeldbo et al.* [1971] in the inversion of occultation data for the Mariner 5 Venus probe, where it was found that significant variations in the attenuation data corresponded to barely noticeable perturbations in

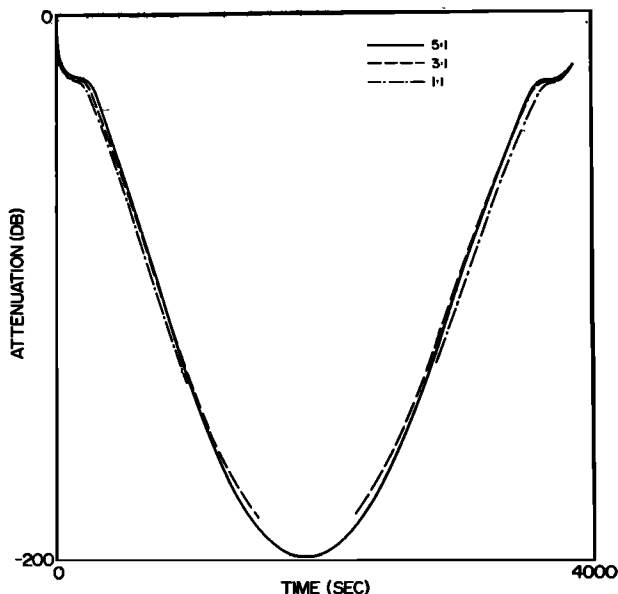


Fig. 7. Comparison of excess path length due to retardation as generated for five models with cloud top temperature held at 250°K and the H_2/He ratio as indicated.

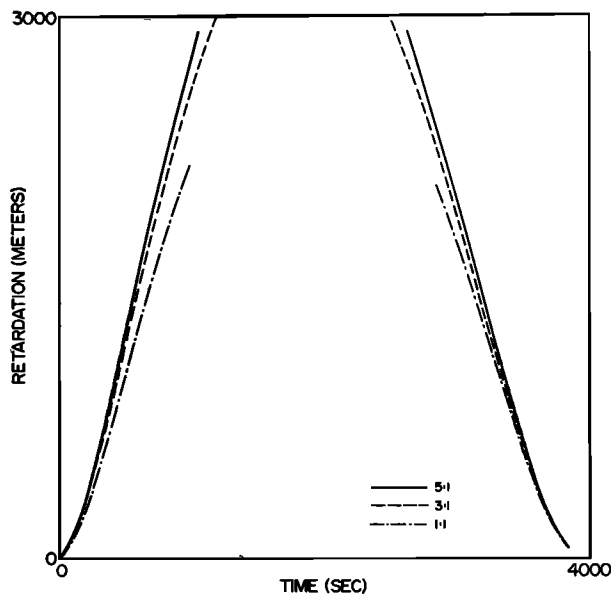


Fig. 9. Comparison of total attenuation as generated for five models, each with a H_2/He ratio as indicated and with cloud top temperature held at 250°K.

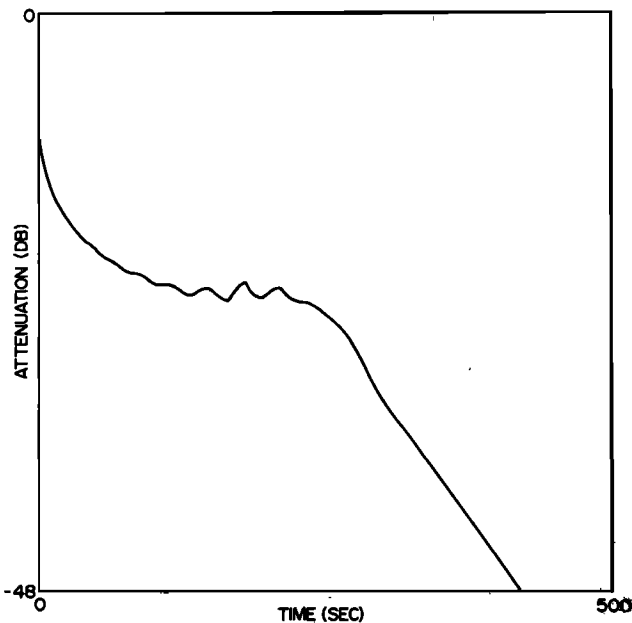


Fig. 10. Detailed look at the record of Figure 5 showing the fine structure of the 'flash.'

the temperature profile.) The observed bump in the attenuation record is therefore a potential tool for measuring the height of the convective zone, under the assumption that a 2-dB variation is detectable and horizontal gradients in the Jovian atmosphere do not wash out the effect.

It is interesting to note that if the radio signal were visible radiation, the bump would probably be described as a 'flash,' and flashes were in fact observed high in the atmosphere of Jupiter when the planet occulted Beta Scorpii in 1971. Those flashes could perhaps also have arisen from density variations.

CONCLUSIONS

A preliminary computer simulation of the Pioneer 10 occultation experiment has been performed by using model Jovian atmospheres developed by Hogan, Encrenaz, and Gautier in conjunction with Pioneer 10 trajectory data supplied by the Pioneer Project manager's office. Analysis of the results indicates that the useful depth of penetration of the experiment will be determined by ammonia absorption rather

than superrefractivity, that, in fact, the Jovian atmosphere is not superrefractive above the visible cloud deck, but that attenuation due to ammonia absorption can be of the order of 200 dB near the cloud deck.

The experiment appears to be far more sensitive to variations in the cloud top temperature than in the hydrogen-helium compositional ratios and will probably prove to be a useful temperature sensor down to those levels in which the signal is detectable. It would appear that the experiment is less useful in determining the H_2/He ratio.

Finally, it appears that the attenuation record may provide information as to the depth of the convective zone if the feature that appeared in the simulations is in fact real and is not an experimental artifact.

Acknowledgments. The author would like to thank J. S. Hogan for providing the Jupiter model atmospheres and for his generous help and guidance throughout this research. Thanks are also extended to the Pioneer project manager for the Pioneer 10 trajectory data. This work was performed while the author was a National Research Council Resident Research Associate at the NASA Goddard Institute for Space Studies in New York City.

REFERENCES

- Fjeldbo, G., A. Kliore, and V. R. Eshleman, The neutral atmosphere of Venus as studied with the Mariner 5 radio occultation experiments, *Astron. J.*, 76, 1387, 1971.
- Hogan, J. S., R. W. Stewart, S. I. Rasool, and L. H. Russell, Results of the Mariner 6 and 7 Mars occultation experiments, *NASA Tech. Note D-6683*, 1972.
- Kliore, A., D. L. Cain, G. S. Levy, V. R. Eshleman, G. Fjeldbo, and F. D. Drake, Occultation experiment: Results of the first direct measurement of Mars atmosphere and ionosphere, *Science*, 158, 3689, 1965.
- Kliore, A., G. S. Levy, D. L. Cain, G. Fjeldbo, and S. I. Rasool, Atmosphere and ionosphere of Venus from the Mariner 5 S-band radio occultation measurement, *Science*, 158, 3809, 1967.
- Kliore, A., G. Fjeldbo, B. L. Seidel, and S. I. Rasool, Mariner 6 and 7: Radio occultation measurements of the atmosphere of Mars, *Science*, 166, 3910, 1969.
- Kliore, A., D. L. Cain, G. Fjeldbo, B. L. Seidel, and S. I. Rasool, Mariner 9 S-band Martian occultation experiment: Initial results on the atmosphere and topography of Mars, *Science*, 175, 4019, 1972.
- Mariner Stanford Group, Venus: Ionosphere and atmosphere as measured by dual-frequency radio occultation of Mariner 5, *Science*, 158, 3809, 1967.

(Received November 19, 1973;
accepted January 25, 1974.)